Acta Cryst C STRUCTURAL CHEMISTRY
ISSN 2053-2296

The 2′-deoxyribofuranoside of 3-phenyltetrahydropyrimido[4,5-*c*]pyridazin-7-one: a bicyclic nucleoside with sugar residues in *N* and *S* conformations, and its molecular recognition

Hui Mei,[a] Simone Budow-Busse,[a] Dasharath Kondhare,[a] Henning Eickmeier,[b] Hans Reuter[b] and Frank Seela[a,c]*

[a]Laboratory of Bioorganic Chemistry and Chemical Biology, Center for Nanotechnology, Heisenbergstrasse 11, 48149 Münster, Germany, [b]Anorganische Chemie II, Institut für Chemie neuer Materialien, Universität Osnabrück, Barbarastrasse 7, 49069 Osnabrück, Germany, and [c]Laboratorium für Organische und Bioorganische Chemie, Institut für Chemie neuer Materialien, Universität Osnabrück, Barbarastrasse 7, 49069 Osnabrück, Germany. *Correspondence e-mail: frank.seela@uni-osnabrueck.de

Received 13 April 2022
Accepted 2 June 2022

Edited by E. Y. Cheung, Moderna Inc., USA

Keywords: 2′-deoxyribonucleoside; pyrimido[4,5-c]pyridazine; pK_a value; crystal structure; hydrogen bonding; base pair.

CCDC reference: 2176720

Supporting information: this article has supporting information at journals.iucr.org/c

The title compound 3-phenyltetrahydropyrimido[4,5-*c*]pyridazine 2′-deoxyribonucleoside [systematic name: 6-(2-deoxy-β-D-*erythro*-pentofuranosyl)-5,6,7,8-tetrahydro-3-phenylpyrimido[4,5-*c*]pyridazin-7-one monohydrate, $C_{17}H_{18}N_4O_4\cdot H_2O$, **1**] shows two conformations in the crystalline state and the two conformers (**1a** and **1b**) adopt different sugar puckers. The sugar residue of **1a** shows a C2′-*endo* *S*-type conformation, while **1b** displays a C3′-*endo* *N*-type sugar pucker. Both conformers adopt similar *anti* conformations around the N-glycosylic bonds, with $\chi = -97.5\ (3)^\circ$ for conformer **1a** and $\chi = -103.8\ (3)^\circ$ for conformer **1b**. The extended crystalline network is stabilized by several intermolecular hydrogen bonds involving nucleoside and water molecules. The nucleobases and phenyl substituents of the two conformers (**1a** and **1b**) are stacked and display a reverse alignment. A Hirshfeld surface analysis supports the hydrogen-bonding pattern, while curvedness surfaces visualize the stacking interactions of neighbouring molecules. The recognition face of nucleoside **1** for base-pair formation mimics that of 2′-deoxythymidine. Nucleoside **1** shows two pK_a values: 1.8 for protonation and 11.2 for deprotonation. DNA oligonucleotides containing nucleoside **1** were synthesized and hybridized with complementary DNA strands. Nucleoside **1** forms a stable base pair with dA which is as stable as the canonical dA–dT pair. The bidentate **1**–dA base pair is strengthened by a third hydrogen bond provided by the dA analogue 3-bromopyrazolo[3,4-*d*]-pyrimidine-4,6-diamine 2′-deoxyribofuranoside (**4**). By this, duplex stability is increased and the suggested base-pairing patterns are supported.

1. Introduction

Nucleosides with artificial nucleobases offer new functionalities not existing in the canonical constituents of DNA and RNA. Alteration of the nitrogen pattern and functionalization with additional substituents are methods to change molecular recognition and base-pair stability. Artificial nucleosides were used to probe interactions in DNA and RNA, or with proteins and other biomolecules. In addition, DNA is utilized in materials science for information storage or as a nanomaterial (Meiser *et al.*, 2020). Entirely new base pairs were constructed to expand the repertoire of nucleic acid applications (Hirao *et al.*, 2012). Often, only minor structural changes are needed to achieve these objectives.

Pyrimido[4,5-*c*]pyridazine 2′-deoxyribonucleoside **1** [Scheme 1 shows nucleoside **1** and structurally related compounds, with the recognition sites according to dT (red) and dC (blue)] can

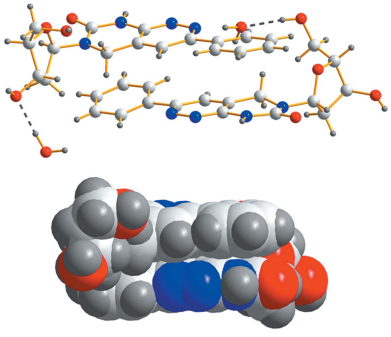

serve as a mimic for 2′-deoxythymidine (dT). Nucleoside **1** shows ambiguous base-pair recognition (Topal & Fresco, 1976). Nevertheless, it is able to distinguish between canonical purine and pyrimidine nucleosides with a preference for complementary 2′-deoxyadenosine (dA) (Mei *et al.*, 2015). This is contrary to the related nucleosides **2** and **3**, which display the recognition face of 2′-deoxycytidine (dC). Compound **1** has a strong structural relationship to pyrrolo-dC (**2**) and imidazolo-dC (**3**) (see Scheme 1), and is decorated with a phenyl ring, as is the case for **2** and **3** (Hudson & Ghorbani-Choghamarani, 2007; Mei *et al.*, 2014). A 3-methylpyrimido[4,5-*c*]pyridazine nucleoside (Loakes *et al.*, 2003*a*,*b*) and a phenylethyl derivative were reported previously (Mieczkowski *et al.*, 2016). Nucleoside **1** was synthesized in our laboratory and incorporated into DNA oligonucleotides employing phosphoramidite chemistry and solid-phase oligonucleotide synthesis (Mei *et al.*, 2015). Chemical synthesis of DNA oligonucleotides has several advantages over triphosphate incorporation catalyzed by polymerases, especially when modified nucleosides are used. Modified nucleosides are often not sufficiently accepted by DNA polymerases and therefore chain elongation succeeds only in low yields or is terminated (Hollenstein, 2012). DNA oligonucleotide synthesis with nucleoside phosphoramidites can be performed even with highly modified nucleosides and is a standard method in the field of nucleic chemistry.

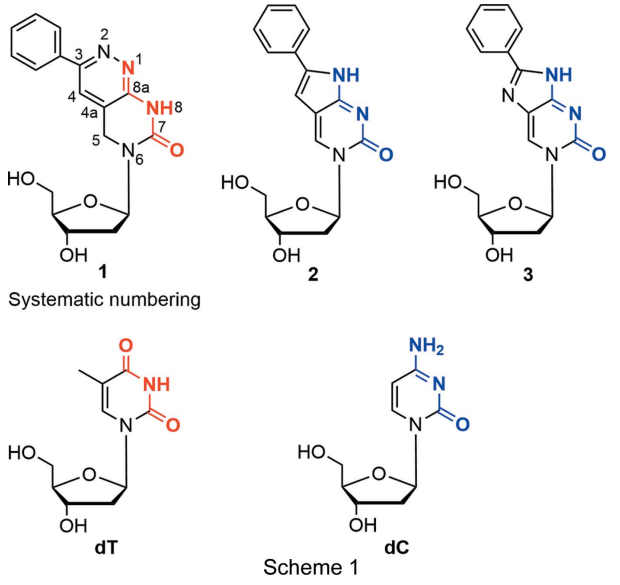

Scheme 1

To obtain detailed information on its conformation and crystal packing in the solid state, a single-crystal X-ray analysis of nucleoside **1** was performed. A Hirshfeld surface analysis was carried out to visualize the packing interactions. DNA oligonucleotides containing phenylpyrimido[4,5-*c*]pyridazine nucleoside **1** were synthesized and hybridization experiments were performed to strengthen the bidentate **1**–dA base pair (Mei *et al.*, 2015) by replacement with a tridentate base pair employing 3-bromopyrazolo[3,4-*d*]pyrimidine-4,6-diamine 2′-deoxyribofuranoside, **4** (Seela & Becher, 2001; He *et al.*, 2003), as dA surrogate.

Table 1
Experimental details.

Crystal data	
Chemical formula	$C_{17}H_{18}N_4O_4·H_2O$
M_r	360.37
Crystal system, space group	Orthorhombic, $P2_12_12_1$
Temperature (K)	100
a, b, c (Å)	7.2057 (3), 11.0792 (4), 41.2346 (16)
V (Å^3)	3291.9 (2)
Z	8
Radiation type	Mo $K\alpha$
μ (mm^{-1})	0.11
Crystal size (mm)	0.19 × 0.16 × 0.09
Data collection	
Diffractometer	Bruker APEXII CCD
Absorption correction	Multi-scan (*SADABS*; Bruker, 2008)
T_{min}, T_{max}	0.979, 0.991
No. of measured, independent and observed [$> I > 2\sigma(I)$] reflections	91832, 4528, 3773
R_{int}	0.118
(sin $\theta/\lambda)_{max}$ (Å^{-1})	0.661
Refinement	
$R[F^2 > 2\sigma(F^2)]$, $wR(F^2)$, S	0.045, 0.096, 1.07
No. of reflections	4528
No. of parameters	473
H-atom treatment	H atoms treated by a mixture of independent and constrained refinement
$\Delta\rho_{max}$, $\Delta\rho_{min}$ (e Å^{-3})	0.27, −0.31
Absolute structure	Established by known chemical absolute configuration

computer programs: *APEX2* (Bruker, 2008), *SAINT* (Bruker, 2008), *SHELXTL* (Sheldrick, 2008), *DIAMOND* (Brandenburg, 2005), *SHELXTL* (Sheldrick, 2008) and *PLATON* (Spek, 2020).

2. Experimental

2.1. Synthesis and crystallization of 1

Nucleoside **1** was synthesized as described previously (Mei *et al.*, 2015). Colourless crystals of **1** were obtained from a hot methanol/water mixture (m.p. 450 K). For the X-ray crystallographic analysis, a single crystal was mounted on a MiTeGen Micro-Mounts fibre in a thin smear of oil.

2.2. Refinement

Crystal data, data collection and structure refinement details are summarized in Table 1. The known configuration of the parent molecule was used to define the enantiomer employed in the refined model. In the absence of suitable anomalous scattering, Friedel equivalents could not be used to determine the absolute structure. Refinement of the Flack (1983) parameter led to inconclusive values for this parameter [0.0 (6)]. All H atoms were found in a difference Fourier synthesis. In order to maximize the data/parameter ratio, the H atoms were placed in geometrically idealized positions, with C—H = 0.95–1.00 Å, and were constrained to ride on their parent atoms, with U_{iso}(H) = 1.2U_{eq}(C) = U_{eq}(N). The hydroxy groups were refined as groups allowed to rotate but not tip, with O—H = 0.84 Å and U_{iso}(H) = 1.5U_{eq}(O).

Table 2
Selected geometric parameters (Å, °).

C11*C*—C13	1.483 (4)	C21*C*—C23	1.486 (4)
N16—C11′	1.457 (3)	N26—C21′	1.448 (3)
N16—C15—C14*A*	112.7 (2)	N26—C25—C24*A*	112.8 (2)
C16*C*—C11*C*—C13—N12	−16.1 (4)	C26*C*—C21*C*—C23—N22	−6.8 (4)
C17—N16—C11′—O14′	−97.5 (3)	C27—N26—C21′—O24′	−103.8 (3)
C13′—C14′—C15′—O15′	177.20 (19)	C23′—C24′—C25′—O25′	54.4 (3)

3. Results and discussion

3.1. Molecular geometry and conformation of 1

The crystals of phenylpyrimido[4,5-*c*]pyridazine nucleoside **1** are orthorhombic with the space group $P2_12_12_1$. There are two molecules of **1** in the asymmetric unit, denoted as conformer **1a** and conformer **1b**. As shown in Fig. 1, each conformer is connected to a water molecule *via* hydrogen bonding. Selected geometric parameters are summarized in Table 2.

The orientation of the nucleobase relative to the sugar residue (*syn–anti*) is defined by the torsion angle χ(O4′—C1′—N9—C4) (IUPAC–IUB Joint Commission on Biochemical Nomenclature, 1983), and the preferred conformation around the N-glycosidic bond is *anti* for canonical purine 2′-deoxyribonucleosides (Saenger, 1984). For pyrimido[4,5-*c*]-pyridazine nucleoside **1**, the torsion angle χ(O4′—C1′—N6—C7) is defined in analogy to natural nucleosides, as this molecule can be considered as a purine nucleoside analogue. Both conformers of molecule **1** adopt similar *anti* conformations, with χ = −97.5 (3)° for conformer **1a** and χ = −103.8 (3)° for conformer **1b**.

The pyridazine rings of **1a** and **1b** are nearly planar. For **1a**, the deviations of the ring atoms (N11/N12/C13/C14/C14*A*/C18*A*) from the least-squares plane range from 0.013 (2) Å for atom C14*A* to −0.013 (2) Å for atom C18*A*, with an r.m.s. deviation of 0.0091 Å. In the case of conformer **1b**, the r.m.s. deviation of the ring atoms from their calculated least-squares planes is 0.0216 Å and the range is from 0.032 (2) Å for atom C28*A* to −0.022 (2) Å for atom C24*A*. The presence of the sp^3-hybridized C15/C25 atom causes a displacement of the C atom from the mean plane in both conformers compared to a reduced pyrimidine moiety. In **1a**, atom C15 is displaced by 0.081 (4) Å from the mean plane, while for **1b** the displacement of atom C25 is −0.134 (4) Å. The corresponding N6—C5—C4*A* bond angle is 112.7 (2)° for **1a** and 112.8 (2)° for **1b**.

In both conformers, the pyridazine ring and the phenyl substituent are slightly tilted with respect to each other, with C16*C*—C11*C*—C13—N12 = −16.1 (4)° for **1a** and C26*C*—C21*C*—C23—N22 = −6.8 (4)° for **1b**. The C3—C1*C* bond connecting the phenyl moiety with the pyridazine ring is almost identical for both conformers [C13—C11*C* = 1.483 (4) Å for **1a** and C23—C21*C* = 1.486 (4) Å for **1b**]. Also, the N6—C1′ bond connecting the nucleobase and the sugar moiety is of comparable length [1.457 (3) Å for **1a** and 1.448 (3) Å for **1b**].

The most pronounced differences between conformers **1a** and **1b** concern the conformation of the sugar moiety. The sugar moiety of nucleosides can adopt two principal puckering modes, namely, C3′-*endo* (*N*) and C2′-*endo* (*S*), corresponding to the major dislocation of C3′ or C2′ from the median plane of C1′—O4′—C4′ (Altona & Sundaralingam, 1972; Saenger, 1984). For canonical 2′-deoxyribonucleosides, the preferred sugar conformation is C2′-*endo*. Moreover, the torsion angle γ(O5′—C5′—C4′—C3′) characterizes the orientation of the exocyclic 5′-hydroxy group relative to the sugar moiety (Saenger, 1984). The 2′-deoxyribose ring of **1a** also adopts a C2′-*endo* *S*-type conformation (C3′-*exo*–C2′-*endo*, ${}_3T^2$), with a pseudorotational phase angle P = 182.7 (2)° and a maximum amplitude τ_m = 33.9 (1)°. The conformation about the C4′—

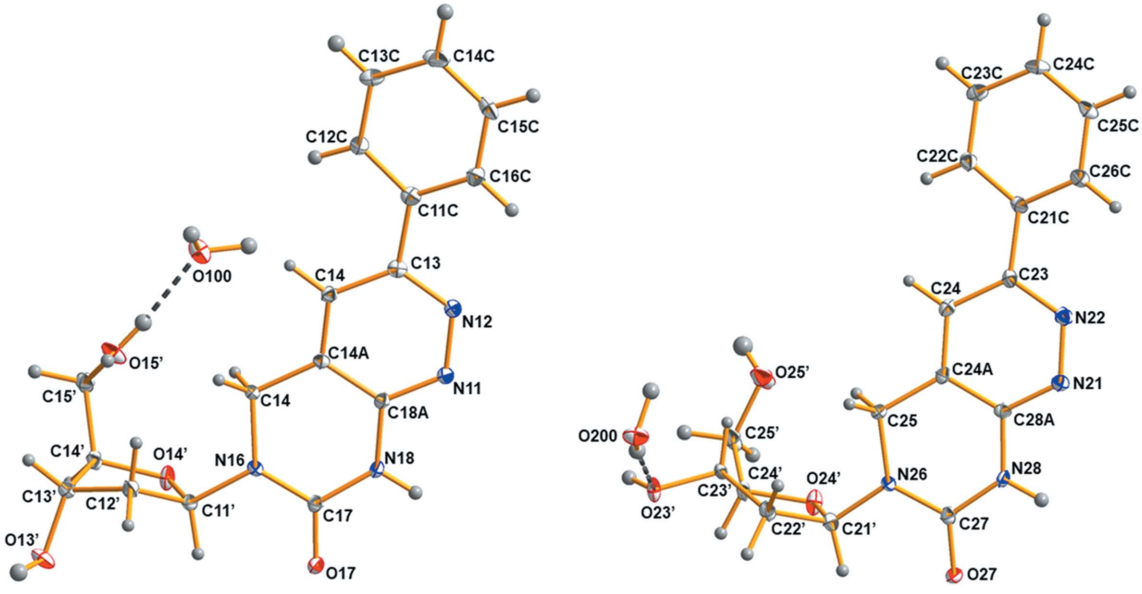

Figure 1
Perspective views and the atom-numbering schemes of conformers **1a** and **1b**, each forming a hydrogen bond to a water molecule (dashed line). Displacement ellipsoids are drawn at the 50% probability level.

Table 3
Hydrogen-bond geometry (Å, °).

D—H···A	D—H	H···A	D···A	D—H···A
N18—H18N···O27^{i}	0.88	1.92	2.773 (3)	162
O13′—H13O···O17^{ii}	0.84	2.15	2.968 (3)	166
O15′—H15O···O100	0.84	1.91	2.736 (2)	169
O100—H101···O15′^{iii}	0.96	1.86	2.781 (3)	160
O100—H100···N22	0.96	1.99	2.946 (3)	175
N28—H28N···O17^{iv}	0.88	1.95	2.823 (3)	173
O23′—H23O···N11^{v}	0.84	2.05	2.846 (3)	158
O25′—H25O···O200^{vi}	0.84	1.90	2.721 (3)	164
O200—H201···O24′^{vii}	0.96	1.84	2.801 (3)	175
O200—H200···O23′	0.96	1.89	2.836 (3)	169

Symmetry codes: (i) $x, y+1, z$; (ii) $x-\frac{1}{2}, -y+\frac{3}{2}, -z+2$; (iii) $x-\frac{1}{2}, -y+\frac{1}{2}, -z+2$; (iv) $x, y-1, z$; (v) $-x+1, y-\frac{1}{2}, -z+\frac{3}{2}$; (vi) $x+1, y, z$; (vii) $-x+1, y+\frac{1}{2}, -z+\frac{3}{2}$.

C5′ bond is antiperiplanar (+*ap*), with the torsion angle γ = 177.2 (2)°. In contrast, a C3′-*endo* *N*-type (C3′-*endo*–C4′-*exo*, $^{3}T_{4}$) sugar conformation is observed for **1b**, with P = 34.6 (2)° and τ_m = 32.4 (1)°. The 5′-hydroxy group of conformer **1b** adopts a synclinal (+*sc*) conformation, with γ = 54.4 (3)°.

The conformational differences of conformers **1a** and **1b**, which mainly concern the sugar moiety (*N versus S* conformation), are probably the consequence of the different hydrogen-bonding sites of the sugar residues to nearby water molecules.

3.2. Hydrogen bonding and molecular packing of 1

The crystalline structure of phenylpyrimido[4,5-*c*]pyridazine nucleoside **1** is stabilized by a heterogeneous network consisting of several intermolecular hydrogen bonds which involve the nucleoside and water molecules (Table 3). The hydrogen bonds formed by the water molecules are particularly important as they stabilize the different sugar conformations of the two conformers (**1a** and **1b**). Notably, conformer **1a** with a C2′-*endo* (*S*) conformation forms a hydrogen bond to nearby water molecules only *via* its 5′-hydroxy group, while the sugar moiety of conformer **1b**, with a C3′-*endo* (*N*) conformation, has multiple contacts to nearby water molecules. This includes the 3′- and 5′-hydroxy groups, and atom O24′ of the furanose ring [for details and symmetry codes, see Table 3 and Fig. 2(*a*)].

Conformers **1a** and **1b** are stacked with a reverse alignment with respect to each other, forming a compact unit. Within this unit, hydrogen-bond formation is not observed between the conformers. As shown in Figs. 2(*a*) and 2(*b*), the phenyl substituent of each conformer faces the pyrimidine ring of the nucleobase of the other conformer. In addition, each sugar residue points towards the other conformer. This is somewhat different to the arrangement in the crystal structure of the closely related 3-methylpyrimido[4,5-*c*]pyridazine nucleoside (Loakes *et al.*, 2003*a*), wherein the sugar units point away from the other conformer (see Fig. S1 in the supporting information).

The arrangement of conformers **1a** and **1b** within the extended crystalline network and the hydrogen-bonding scheme is shown in Fig. 3 and the supporting information (Fig. S2). The two conformers are linked by hydrogen bonds

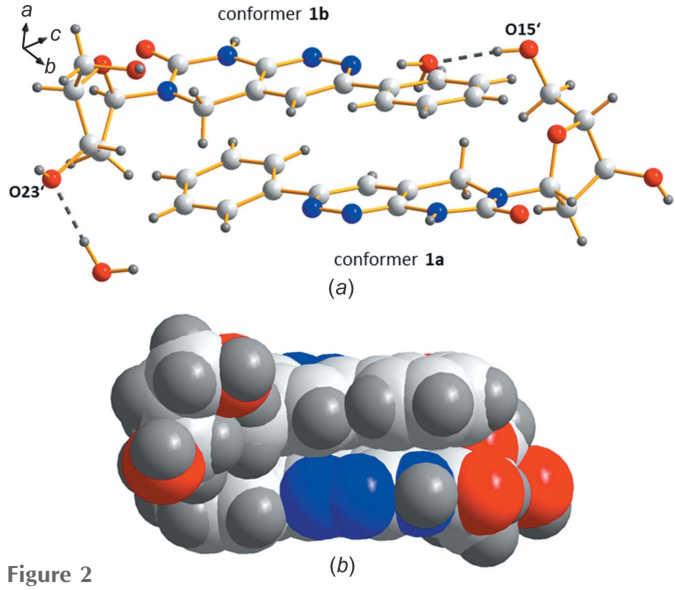

Figure 2
(*a*) Reverse alignment of conformers **1a** and **1b**, and hydrogen bonding to water molecules (dashed lines). (*b*) Space-filling model of a compact unit consisting of conformers **1a** and **1b**.

formed between neighbouring pyrimidine moieties of the other conformer with atom N8 as donor and atom O7 as acceptor (N18—H18N···O27^{i} and N28—H28N···O17^{iv}). Most interestingly, atom O17 of conformer **1a** also functions as an acceptor for a hydrogen bond with the 3′-hydroxy group of another molecule of **1a** (O13′—H13O···O17^{ii}), while this kind of contact is not observed for conformer **1b**. On the other hand, pyridazine atom N22 is the acceptor for a contact to a nearby water molecule (O100—H100···N22), whereas the corresponding atom N12 of conformer **1a** is not involved in hydrogen bonding.

In addition, the arrangement of the nucleobases results in π–π stacking between the phenyl and pyrimido[4,5-*c*]pyridazine rings, as shown in Fig. 3(*a*), with interatomic distances ranging from 3.12 (N12···C24) to 3.69 Å (N16···C25*C*). The π–π interaction of the ring systems is supported by the Hirshfeld surface analysis of nucleoside **1** (see next section).

3.3. Hirshfeld surface analysis of nucleoside 1

The Hirshfeld surface analysis, including three-dimensional (3D) surfaces and two-dimensional (2D) fingerprint plots, provides additional insight into the role of crystal packing forces and visualizes the relative strengths of intermolecular interactions of crystalline compounds. The program *CrystalExplorer* (Version 17; Spackman & Jayatilaka, 2009; Turner *et al.*, 2017) was used to carry out a Hirshfeld surface analysis of phenylpyrimido[4,5-*c*]pyridazine nucleoside **1**, mapped in the $d_{\rm norm}$ range from −0.5 to 1.5 Å, shape index (−1.0 to 1.0 Å) (see Fig. S3 in the supporting information) and curvedness (−4.0 to 0.4 Å), as well as a 2D fingerprint plot analysis. The Hirshfeld surfaces depicted in Figs. 4(*a*)–(*d*) show several deep-red spots representing short contacts, while white surface areas indicate contacts with distances equal to the sum of the van der Waals radii. The red spots correspond to the close O—

H···O and N—H···O contacts of the molecules and confirm the hydrogen-bonding data (Table 3). In addition, the curvedness surfaces show a large and relatively flat green region covering the pyrimido[4,5-*c*]pyridazine nucleobase and the phenyl substituent [Figs. 4(*e*) and 4(*f*)]. This indicates the presence of π–π stacking interactions with neighbouring molecules and fits the crystal packing scheme wherein the heterocyclic nucleobases and the phenyl substituent of the two conformers (**1a** and **1b**) face each other with a reverse orientation [Fig. 2(*a*)].

Fig. 5 shows the overall 2D fingerprint plot of molecule **1** [Fig. 5(*a*)] and the plots resolved into O···H/H···O, N···H/H···N, C···H/H···C and H···H contacts [Figs. 5(*b*)–(*e*)] to highlight the particular atom-pair interactions, together with their relative contributions to the Hirshfeld surface. The proportions of O···H/H···O and N···H/H···N interactions comprise 27.4 and 9.7%, respectively, of the total Hirshfeld surfaces. The H···H and C···H/H···C contacts amount to 52.0 and 4.3%, respectively, and suggest that van der Waals interactions also play a role in the crystal packing of nucleoside **1**.

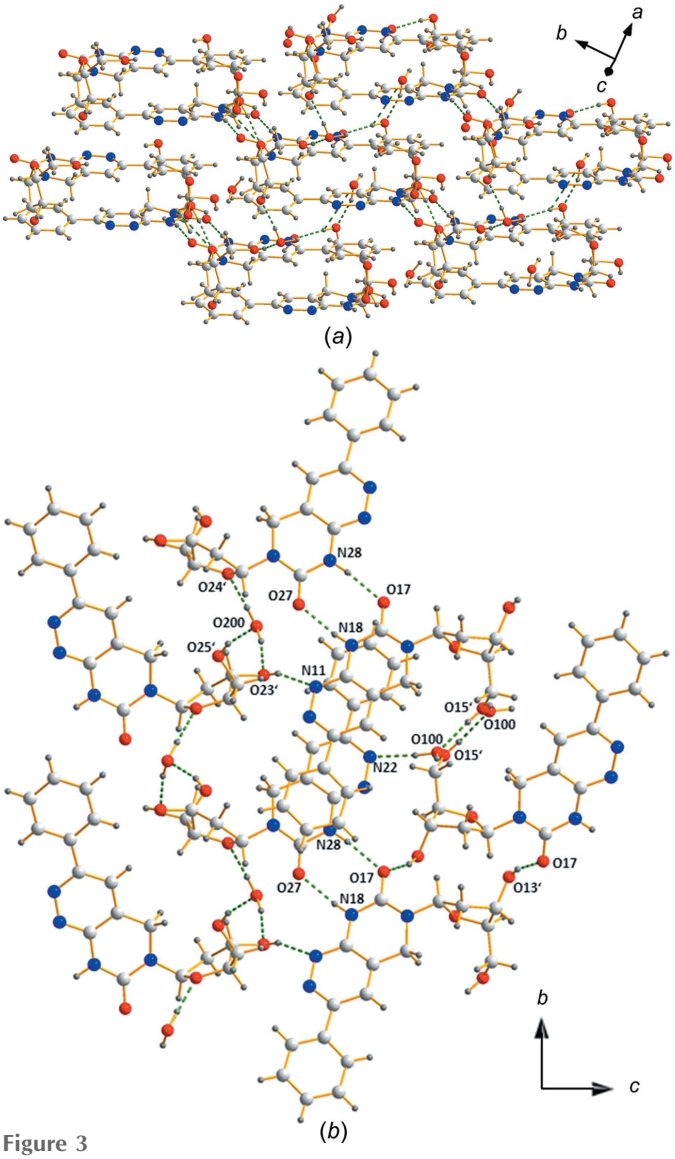

Figure 3
(*a*) Packing of conformers (**1a** and **1b**) within the extended crystalline network. (*b*) Detailed view of the hydrogen-bonding scheme (dashed lines), shown parallel to the *bc* plane.

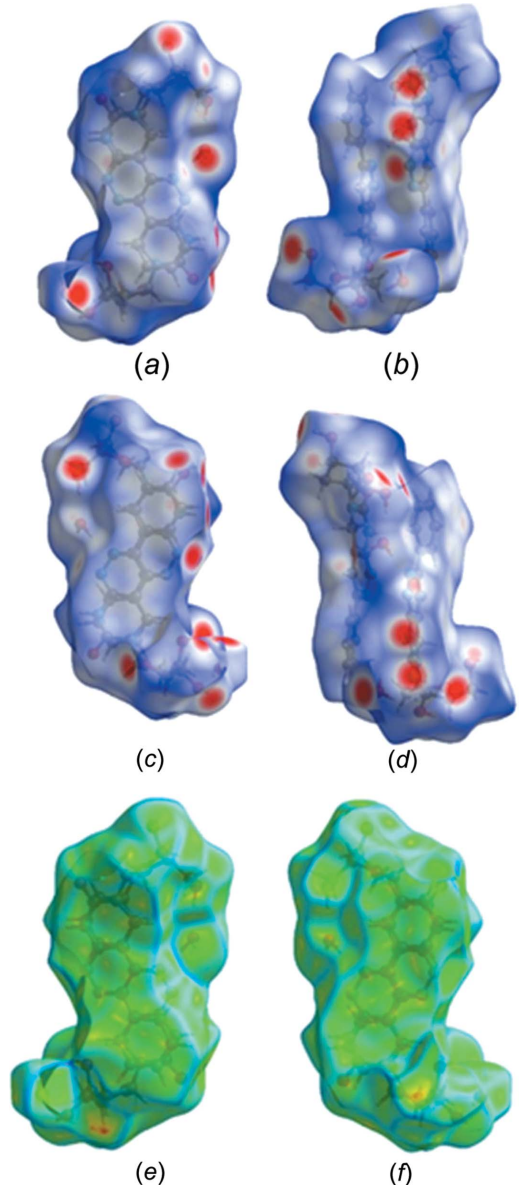

Figure 4
Hirshfeld surfaces of conformers **1a** and **1b** mapped with d_{norm} (0.5 to 1.5 Å), shown in (*a*) front, (*b*)/(*c*) side and (*d*) back views. The curvedness surfaces of the two conformers of nucleosides **1a** and **1b** are shown in (*e*) front and (*f*) back views.

3.4. p*K* values and base pairing

The pK_a values (ionization or dissociation constants) of canonical and modified nucleobases are an important parameter for the prediction of base-pairing properties in terms of their lifetime and stability. Accordingly, the p*K* value of nucleoside **1** was determined and compared to that of dT. For p*K* determination, the spectrophotometric UV titration of **1** was performed and the dependency of a continuously increased pH value and absorption data were plotted against

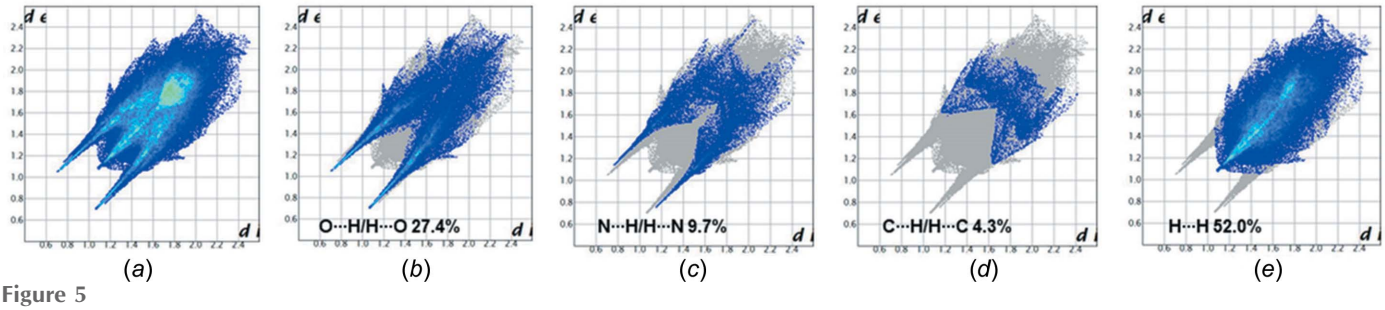

Figure 5
2D fingerprint plots showing the percentage contributions of various interactions to the total Hirshfeld surface area of the two conformers of compound **1**: (*a*) full interactions and resolved contacts; (*b*) O···H/H···O; (*c*) N···H/H···N; (*d*) C···H/H···C; (*e*) H···H.

pH values. To cover the full range of the pH scale, measurements were carried out between pH 12.8 and pH 8.5 [Fig. 6(*a*)], as well as between pH 5.5 and pH 0.7 [Fig. 6(*c*)]. Due to the two-state equilibrium of the protonated and deprotonated species, isosbestic points are observed in the UV spectra [Figs. 6(*a*) and 6(*c*)]. Fig. 6(*b*) displays a pK value of 11.2 for the deprotonation of nucleoside **1**. This is higher than that of dT (9.8) and makes the deprotonation of **1** more difficult. The pK_a value of protonation of **1** was found to be 1.8 [Fig. 6(*d*)]. dT has no pK value in this range. For the protonation of **1**, nitrogen-1 and nitrogen-3 are the possible proton-acceptor sites (Fig. 7). Earlier, it was reported that strong base pairs are formed when the pK value difference (ΔpK) between the acceptor and donor sites of nucleobases is greater than 5 units (Krishnamurthy, 2012). Thus, pK value differences were calculated for the base-pair motifs shown in Fig. 8. Similar

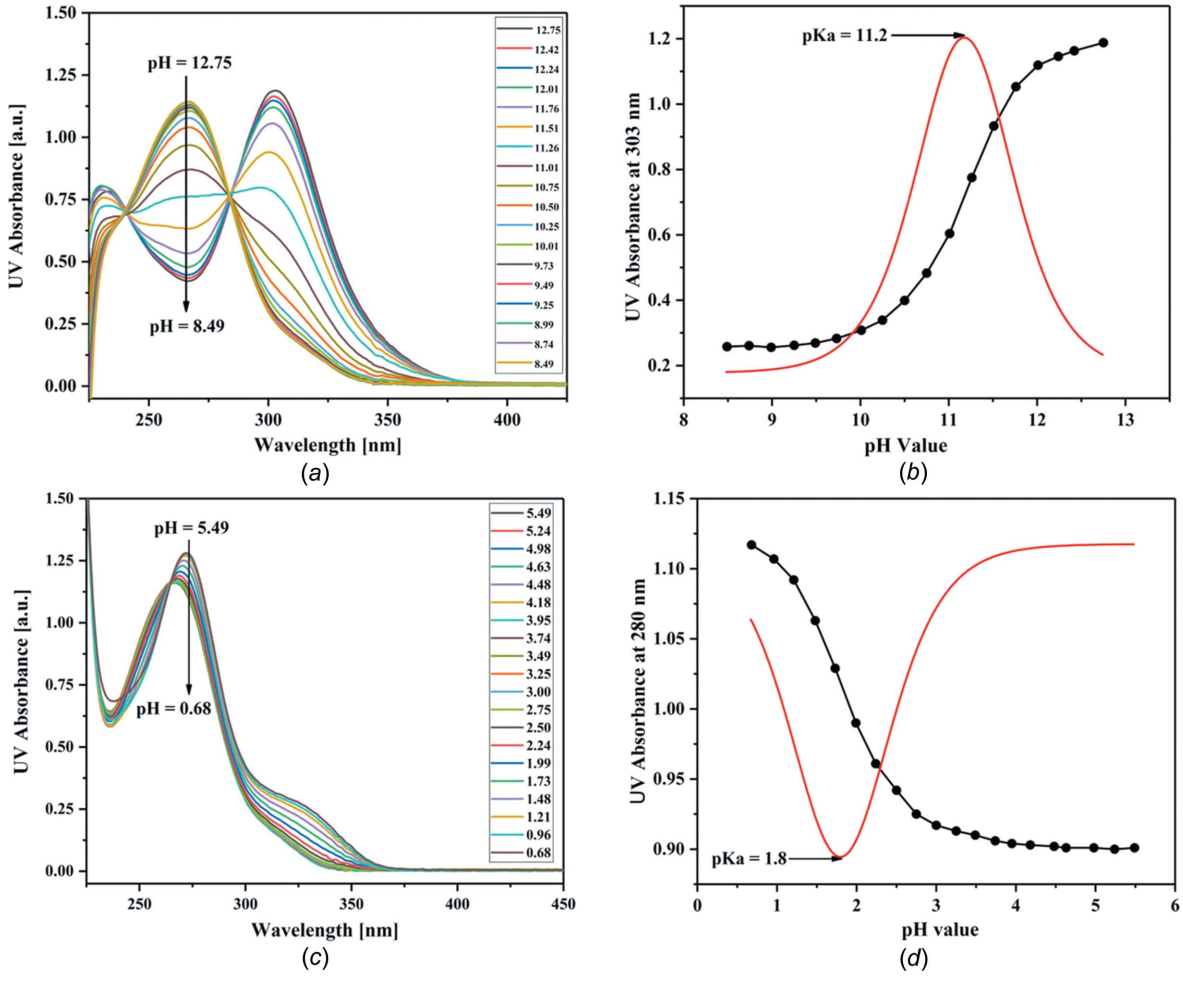

Figure 6
(*a*) pH-dependent UV spectra of **1** measured in phosphate buffer from pH 12.75 to pH 8.49. (*b*) Absorbance of **1** at 303 nm *versus* pH value and its first derivative using data from part (*a*). (*c*) pH-dependent UV spectra of **1** measured in phosphate buffer from pH 5.49 to pH 0.68. (*d*) Absorbance of **1** at 280 nm *versus* pH value and its first derivative using data from part (*c*).

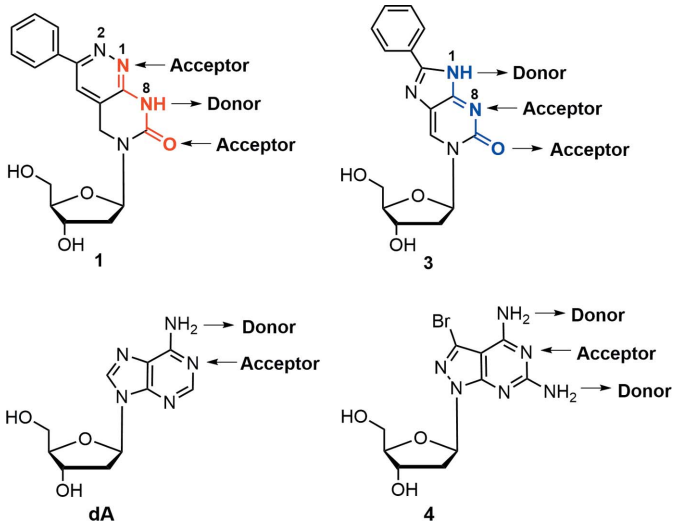

Figure 7
Donor–acceptor pattern of nucleosides **1**, **3**, dA and **4**.

Δp*K* values were found for the **1**–dA and dT–dA base pairs, which supports stable base-pair formation. Base pairing of a related compound with a methyl group instead of the phenyl group was reported previously (Loakes *et al.*, 2003*a*). However, base-pair motifs were not given and p*K* values were not determined.

The X-ray crystal structure of **1** reported in this study unambiguously shows that the H atom is located at nitrogen-8 (pyrimidine ring; Fig. 1) and can act as proton donor for **1**–dA base pairing. This is different to nucleosides **2** and **3**, which carry the H atoms at nitrogen-1 (imidazole/pyrrole ring). According to the shift of the proton-donor site from nitrogen-1 to nitrogen-8, N1 now becomes an acceptor site in nucleoside **1**. This is a consequence of the ring displacement (pyridazine instead of pyrrole or imidazole) and makes nucleoside **1** an analogue of dT, whereas compounds **2** and **3** are analogues of dC (Fig. 7).

The dA–dT base pair can be stabilized when an additional amino group is added at the 2-position of the adenine base (Chazin *et al.*, 1991). These stabilizers make use of the principle of third hydrogen-bond formation. 3-Bromopyrazolo-[3,4-*d*]pyrimidin-4,6-diamine 2′-deoxyribofuranoside, **4**, has been used as a stabilizer for the dA–dT base pair (Seela & Becher, 2001; He *et al.*, 2003). Compared to dA, nucleoside **4** contains an additional amino group at position-2 that can participate in a third hydrogen bond with dT (Figs. 7 and 8). This causes a stabilization of the base pair and increases the thermal stability of DNA (Table 4).

We anticipated that a similar stabilization should take place when nucleoside **1** is part of the **1**–dA base pair. Accordingly, an increased temperature of duplex dissociation (T_m) should be observed. The T_m value is a measure for the stability of a double-stranded DNA and depends on the stability of its base pairs. It is measured spectrophotometrically (UV) at 260 nm and can be followed by the absorbance change with increasing temperature and the transition from double- to single-stranded DNA.

Table 4
T_m values of DNA oligonucleotide duplexes containing base pairs formed by nucleosides **1** and **4**[a].

Duplex	T_m[b] (°C)
5′-d(TAG GTC AAT ACT) (ODN-**1**) 3′-d(ATC CAG TTA TGA) (ODN-**2**)	47
5′-d(TAG GTC 4AT ACT) (ODN-**3**) 3′-d(ATC CAG TTA TGA) (ODN-**2**)	54
5′-d(TAG GTC AAT ACT) (ODN-**1**) 3′-d(ATC CAG 1TA TGA) (ODN-**4**)	47
5′-d(TAG GTC 1AT ACT) (ODN-**5**) 3′-d(ATC CAG 4TA TGA) (ODN-**6**)	50

Notes: (*a*) measured at 260 nm at a concentration of 2 μ*M* + 2 μ*M* single strand at a heating rate of 1 °C min^{-1} in 100 m*M* NaCl, 10 m*M* $MgCl_2$ and 10 m*M* Na cacodylate (pH 7.0). (*b*) T_m values were calculated from the heating curves using the program *Meltwin* (Version 3.0; McDowell & Turner, 1996) and are given with an error of ±5%.

To this end, DNA oligonucleotides ODN-**1** to ODN-**6** were synthesized and hybridization experiments were performed (for experimental details, see the supporting information). The T_m data are summarized in Table 4 and melting profiles are displayed in Fig. S4 in the supporting information. According to the T_m data, a stability increase is observed from 47 °C for the duplex containing the **1**–dA base pair to 50 °C (+3 °C) for the duplex ODN-**5**–ODN-**6** incorporating the **1**–**4** pair. Apparently, a tridentate **1**–**4** base pair is formed. Nevertheless, the increase induced by the **1**–**4** pair is lower than that for the **4**–dT pair (T_m = 54 °C; +7 °C). Obviously, the formation of the third hydrogen bond is less efficient in the **1**–**4** base pair than for the dT pair with **4**. Electronic and geometric properties of the nucleobases including altered stacking interactions might account for this behaviour. Possible base-pairing motifs for the **1**–dA and **1**–**4** pairs are displayed in Fig. 8, together with the motifs of the dT–dA and dT–**4** pairs.

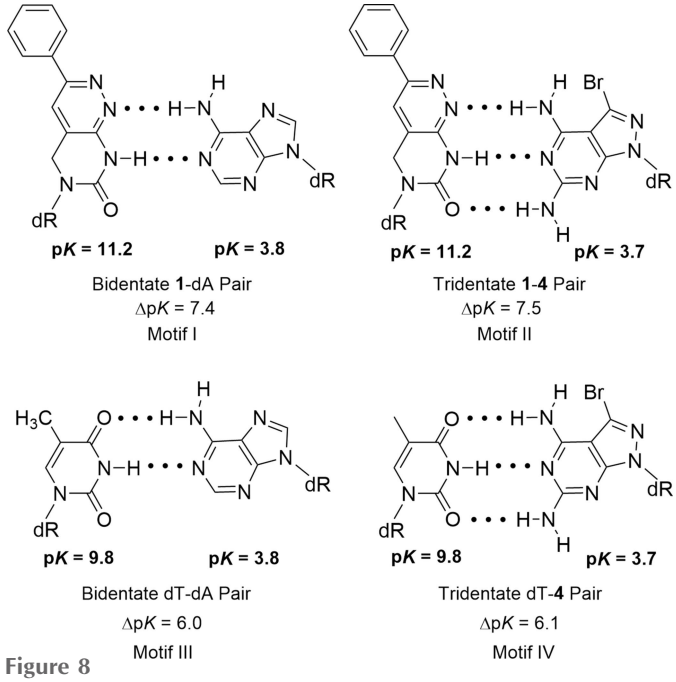

Figure 8
Base-pairing motifs, p*K* values of base-pairing nucleosides and their p*K* value differences (Δp*K*).

4. Conclusion

Phenylpyrimido[4,5-*c*]pyridazine 2′-deoxyribonucleoside **1** forms two conformers (**1a** and **1b**) in the solid state. Conformer **1a** displays a C2′-*endo* *S*-type sugar pucker, whereas conformer **1b** adopts a C3′-*endo* *N*-type conformation. Both conformers show *anti* conformations around the N-glycosylic bonds, with $\chi = -97.5\ (3)^\circ$ for conformer **1a** and $\chi = -103.8\ (3)^\circ$ for conformer **1b**. The extended crystalline structure of nucleoside **1** is stabilized by a heterogeneous hydrogen-bond network involving the nucleoside and water molecules. Conformers **1a** and **1b** are placed opposite each other with a reverse alignment. Strong stacking interactions are observed for the nucleobase and the phenyl ring decorating the heterocycle. A Hirshfeld surface analysis supports the hydrogen-bonding scheme, while the curvedness surfaces visualize the stacking interactions of neighbouring molecules.

Nucleoside **1** mimics the recognition face of dT and is deprotonated under alkaline conditions (**1**: pK_a = 11.2; dT: pK_a = 9.8). DNA duplexes obtained by hybridization of complementary oligonucleotides form a stable **1**–dA base pair that is as stable as the canonical dA–dT pair. The stability of the **1**–dA base pair is increased when the oxo group of **1** participates in a third hydrogen bond. This is the case when dA in the dA–**1** base pair is replaced by the 2-amino stabilizer **4** which provides an additional amino group for tridentate base-pair formation.

Acknowledgements

We thank Mrs Chaitali Kaldate for p*K* determintion and oligonucleotide synthesis and Dr Peter Leonard for critical reading of the manuscript. Funding by ChemBiotech, Münster, Germany, is gratefully acknowledged. Open access funding enabled and organized by Projekt DEAL.

References

Altona, C. & Sundaralingam, M. (1972). *J. Am. Chem. Soc.* **94**, 8205–8212.
Brandenburg, K. (2005). *DIAMOND*. Crystal Impact GbR, Bonn, Germany.
Bruker (2008). *APEX2*, *SAINT* and *SADABS*. Bruker AXS Inc., Madison, Wisconsin, USA.
Chazin, W. J., Rance, M., Chollet, A. & Luepin, W. (1991). *Nucleic Acids Res.* **19**, 5507–5513.
Flack, H. D. (1983). *Acta Cryst.* A**39**, 876–881.
He, J., Becher, G., Budow, S. & Seela, F. (2003). *Nucleosides Nucleotides Nucleic Acids*, **22**, 573–576.
Hirao, I., Kimoto, M. & Yamashige, R. (2012). *Acc. Chem. Res.* **45**, 2055–2065.
Hollenstein, M. (2012). *Molecules*, **17**, 13569–13591.
Hudson, R. H. E. & Ghorbani-Choghamarani, A. (2007). *Synlett*, **2007**, 0870–0873.
IUPAC–IUB Joint Commission on Biochemical Nomenclature (1983). *Eur. J. Biochem.* **131**, 9–15.
Krishnamurthy, R. (2012). *Acc. Chem. Res.* **45**, 2035–2044.
Loakes, D., Brown, D. M., Salisbury, S. A., McDougall, M. G., Neagu, C., Nampalli, S. & Kumar, S. (2003*a*). *Helv. Chim. Acta*, **86**, 1193–1204.
Loakes, D., Brown, D. M., Salisbury, S. A., McDougall, M. G., Neagu, C., Nampalli, S. & Kumar, S. (2003*b*). *Tetrahedron Lett.* **44**, 3387–3389.
McDowell, J. A. & Turner, D. H. (1996). *Biochemistry*, **35**, 14077–14089.
Mei, H., Ingale, S. A. & Seela, F. (2014). *Chem. Eur. J.* **20**, 16248–16257.
Mei, H., Ingale, S. A. & Seela, F. (2015). *Tetrahedron*, **71**, 6170–6175.
Meiser, L. C., Antkowiak, P. L., Koch, J., Chen, W. D., Kohll, A. X., Stark, W. J., Heckel, R. & Grass, R. N. (2020). *Nat. Protoc.* **15**, 86–101.
Mieczkowski, A., Tomczyk, E., Makowska, M. A., Nasulewicz-Goldeman, A., Gajda, R., Woźniak, K. & Wietrzyk, J. (2016). *Synthesis*, **48**, 566–572.
Saenger, W. (1984). In *Principles of Nucleic Acid Structure*, edited by C. R. Cantor. New York: Springer-Verlag.
Seela, F. & Becher, G. (2001). *Nucleic Acids Res.* **29**, 2069–2078.
Sheldrick, G. M. (2008). *Acta Cryst.* A**64**, 112–122.
Spackman, M. A. & Jayatilaka, D. (2009). *CrystEngComm*, **11**, 19–32.
Spek, A. L. (2020). *Acta Cryst.* E**76**, 1–11.
Topal, M. D. & Fresco, J. R. (1976). *Nature (London)*, **263**, 289–293.
Turner, M. J., McKinnon, J. J., Wolff, S. K., Grimwood, D. J., Spackman, P. R., Jayatilaka, D. & Spackman, M. A. (2017). *CrystalExplorer17*. University of Western Australia. https://crystalexplorer.scb.uwa.edu.au/.

supporting information

Acta Cryst. (2022). C**78**, 382-389 [https://doi.org/10.1107/S2053229622005964]

The 2′-deoxyribofuranoside of 3-phenyltetrahydropyrimido[4,5-*c*]pyridazin-7-one: a bicyclic nucleoside with sugar residues in *N* and *S* conformations, and its molecular recognition

Hui Mei, Simone Budow-Busse, Dasharath Kondhare, Henning Eickmeier, Hans Reuter and Frank Seela

Computing details

Data collection: *APEX2* (Bruker, 2008); cell refinement: *SAINT* (Bruker, 2008); data reduction: *SAINT* (Bruker, 2008); program(s) used to solve structure: *SHELXTL* (Sheldrick, 2008); program(s) used to refine structure: *SHELXTL* (Sheldrick, 2008); molecular graphics: *SHELXTL* (Sheldrick, 2008) and *DIAMOND* (Brandenburg, 2005); software used to prepare material for publication: *SHELXTL* (Sheldrick, 2008) and *PLATON* (Spek, 2020).

3-Phenyltetrahydropyrimido[4,5-*c*]pyridazine 2′-deoxyribonucleoside

Crystal data

$C_{17}H_{18}N_4O_4·H_2O$
M_r = 360.37
Orthorhombic, $P2_12_12_1$
Hall symbol: P 2ac 2ab
a = 7.2057 (3) Å
b = 11.0792 (4) Å
c = 41.2346 (16) Å
V = 3291.9 (2) Å^3
Z = 8
$F(000)$ = 1520
D_x = 1.454 Mg m^{-3}
Mo $K\alpha$ radiation, λ = 0.71073 Å
Cell parameters from 9843 reflections
θ = 2.7–24.5°
μ = 0.11 mm^{-1}
T = 100 K
Plate, colourless
0.19 × 0.16 × 0.09 mm

Data collection

Bruker APEXII CCD diffractometer
Radiation source: fine-focus sealed tube
Graphite monochromator
φ and ω scans
Absorption correction: multi-scan (SADABS; Bruker, 2008)
T_{min} = 0.979, T_{max} = 0.991
91832 measured reflections
4528 independent reflections
3773 reflections with $> I > 2\sigma(I)$
R_{int} = 0.118
θ_{max} = 28.0°, θ_{min} = 2.9°
h = −9→9
k = −11→14
l = −54→54

Refinement

Refinement on F^2
Least-squares matrix: full
$R[F^2 > 2\sigma(F^2)]$ = 0.045
$wR(F^2)$ = 0.096
S = 1.07
4528 reflections
473 parameters
0 restraints
Primary atom site location: structure-invariant direct methods
Secondary atom site location: difference Fourier map

Hydrogen site location: inferred from neighbouring sites
H atoms treated by a mixture of independent and constrained refinement
$w = 1/[\sigma^2(F_o^2) + (0.0414P)^2 + 1.187P]$ where $P = (F_o^2 + 2F_c^2)/3$
$(\Delta/\sigma)_{max} = 0.001$
$\Delta\rho_{max} = 0.27$ e Å^{-3}
$\Delta\rho_{min} = -0.31$ e Å^{-3}
Absolute structure: Established by known chemical absolute configuration

Special details

Geometry. All e.s.d.'s (except the e.s.d. in the dihedral angle between two l.s. planes) are estimated using the full covariance matrix. The cell e.s.d.'s are taken into account individually in the estimation of e.s.d.'s in distances, angles and torsion angles; correlations between e.s.d.'s in cell parameters are only used when they are defined by crystal symmetry. An approximate (isotropic) treatment of cell e.s.d.'s is used for estimating e.s.d.'s involving l.s. planes.

Refinement. Refinement of F^2 against ALL reflections. The weighted *R*-factor *wR* and goodness of fit *S* are based on F^2, conventional *R*-factors *R* are based on *F*, with *F* set to zero for negative F^2. The threshold expression of $F^2 > \sigma(F^2)$ is used only for calculating *R*-factors(gt) *etc*. and is not relevant to the choice of reflections for refinement. *R*-factors based on F^2 are statistically about twice as large as those based on *F*, and *R*- factors based on ALL data will be even larger.

Fractional atomic coordinates and isotropic or equivalent isotropic displacement parameters (Å^2)

	x	*y*	*z*	U_{iso}*/U_{eq}
C11C	0.1273 (3)	0.1164 (2)	0.86156 (6)	0.0122 (5)
C12C	0.1019 (4)	0.0262 (2)	0.88477 (6)	0.0168 (6)
H12C	0.1304	0.0424	0.9068	0.020*
C13C	0.0357 (4)	−0.0868 (3)	0.87604 (7)	0.0226 (7)
H13C	0.0180	−0.1469	0.8922	0.027*
C14C	−0.0046 (4)	−0.1126 (3)	0.84406 (7)	0.0210 (6)
H14C	−0.0495	−0.1901	0.8381	0.025*
C15C	0.0209 (4)	−0.0242 (3)	0.82060 (6)	0.0167 (6)
H15C	−0.0057	−0.0416	0.7985	0.020*
C16C	0.0849 (4)	0.0891 (2)	0.82921 (6)	0.0147 (6)
H16C	0.1004	0.1491	0.8130	0.018*
N11	0.3292 (3)	0.41735 (19)	0.85314 (5)	0.0112 (4)
N12	0.2625 (3)	0.30591 (19)	0.84694 (5)	0.0119 (5)
C13	0.1985 (3)	0.2372 (2)	0.87082 (6)	0.0111 (5)
C14	0.2023 (3)	0.2773 (2)	0.90351 (6)	0.0110 (5)
H14	0.1567	0.2274	0.9205	0.013*
C14A	0.2721 (3)	0.3878 (2)	0.90999 (6)	0.0104 (5)
C15	0.2906 (4)	0.4370 (2)	0.94371 (6)	0.0120 (5)
H15E	0.1740	0.4215	0.9557	0.014*
H15D	0.3919	0.3937	0.9550	0.014*
N16	0.3298 (3)	0.56673 (19)	0.94420 (5)	0.0117 (5)
C17	0.4030 (4)	0.6273 (2)	0.91836 (6)	0.0110 (5)
O17	0.4677 (3)	0.73036 (16)	0.92069 (4)	0.0149 (4)
N18	0.3986 (3)	0.5716 (2)	0.88878 (5)	0.0125 (5)
H18N	0.4416	0.6117	0.8720	0.019*
C18A	0.3315 (3)	0.4570 (2)	0.88350 (6)	0.0097 (5)
C11′	0.3522 (4)	0.6207 (2)	0.97618 (6)	0.0124 (5)
H11′	0.3774	0.7089	0.9736	0.015*
C12′	0.1876 (4)	0.6044 (2)	0.99892 (6)	0.0126 (5)
H12A	0.1022	0.6743	0.9977	0.015*

H12B	0.1179	0.5298	0.9937	0.015*
C13′	0.2784 (4)	0.5957 (2)	1.03218 (6)	0.0124 (5)
H13′	0.2013	0.5469	1.0475	0.015*
O13′	0.3197 (3)	0.71160 (17)	1.04531 (5)	0.0203 (4)
H13O	0.2239	0.7405	1.0539	0.030*
C14′	0.4620 (4)	0.5328 (2)	1.02456 (6)	0.0124 (5)
H14′	0.5604	0.5632	1.0396	0.015*
O14′	0.5082 (2)	0.56537 (17)	0.99174 (4)	0.0144 (4)
C15′	0.4451 (4)	0.3977 (2)	1.02795 (6)	0.0146 (6)
H15A	0.4125	0.3778	1.0506	0.018*
H15B	0.3434	0.3686	1.0138	0.018*
O15′	0.6133 (3)	0.33672 (18)	1.01940 (5)	0.0187 (4)
H15O	0.5917	0.2868	1.0045	0.028*
O100	0.4971 (3)	0.17289 (17)	0.97409 (4)	0.0181 (4)
H101	0.3678	0.1520	0.9737	0.027*
H100	0.5383	0.1635	0.9521	0.027*
C21C	0.7560 (4)	0.3512 (2)	0.89090 (6)	0.0114 (5)
C22C	0.8280 (4)	0.4273 (2)	0.86712 (6)	0.0142 (5)
H22C	0.8285	0.4018	0.8451	0.017*
C23C	0.8992 (4)	0.5400 (2)	0.87517 (6)	0.0159 (6)
H23C	0.9485	0.5908	0.8587	0.019*
C24C	0.8984 (4)	0.5781 (2)	0.90713 (6)	0.0162 (6)
H24C	0.9470	0.6551	0.9127	0.019*
C25C	0.8264 (4)	0.5037 (2)	0.93095 (6)	0.0150 (6)
H25C	0.8245	0.5302	0.9529	0.018*
C26C	0.7569 (4)	0.3909 (2)	0.92312 (6)	0.0133 (5)
H26C	0.7097	0.3401	0.9397	0.016*
N21	0.5765 (3)	0.0444 (2)	0.90156 (5)	0.0140 (5)
N22	0.6355 (3)	0.1576 (2)	0.90698 (5)	0.0137 (5)
C23	0.6818 (3)	0.2301 (2)	0.88234 (6)	0.0108 (5)
C24	0.6575 (4)	0.1919 (2)	0.85004 (6)	0.0119 (5)
H24	0.6846	0.2449	0.8326	0.014*
C24A	0.5947 (4)	0.0782 (2)	0.84413 (6)	0.0110 (5)
C25	0.5540 (4)	0.0311 (2)	0.81091 (6)	0.0123 (5)
H25D	0.4524	0.0791	0.8012	0.015*
H25E	0.6654	0.0415	0.7971	0.015*
N26	0.5008 (3)	−0.09635 (19)	0.81099 (5)	0.0121 (4)
C27	0.4895 (4)	−0.1679 (2)	0.83793 (6)	0.0126 (5)
O27	0.4581 (3)	−0.27703 (16)	0.83627 (4)	0.0177 (4)
N28	0.5126 (3)	−0.1135 (2)	0.86718 (5)	0.0149 (5)
H28N	0.4941	−0.1572	0.8847	0.022*
C28A	0.5630 (4)	0.0056 (2)	0.87133 (6)	0.0116 (5)
C21′	0.4844 (4)	−0.1552 (2)	0.77978 (6)	0.0139 (6)
H21′	0.4342	−0.2385	0.7830	0.017*
C22′	0.3656 (4)	−0.0891 (3)	0.75456 (6)	0.0146 (6)
H22A	0.2774	−0.1454	0.7441	0.017*
H22B	0.2945	−0.0228	0.7648	0.017*
C23′	0.5029 (4)	−0.0395 (2)	0.72989 (6)	0.0118 (5)

H23′	0.5416	0.0441	0.7360	0.014*
O23′	0.4186 (3)	−0.03919 (18)	0.69867 (4)	0.0156 (4)
H23O	0.5010	−0.0327	0.6844	0.023*
O24′	0.6678 (3)	−0.16308 (17)	0.76598 (4)	0.0159 (4)
C24′	0.6665 (4)	−0.1255 (2)	0.73252 (6)	0.0140 (6)
H24′	0.6434	−0.1973	0.7184	0.017*
C25′	0.8534 (4)	−0.0731 (3)	0.72456 (6)	0.0197 (6)
H25A	0.9512	−0.1338	0.7289	0.024*
H25B	0.8583	−0.0516	0.7013	0.024*
O25′	0.8859 (3)	0.0315 (2)	0.74372 (4)	0.0268 (5)
H25O	0.9598	0.0776	0.7340	0.040*
O200	0.1440 (3)	0.14220 (17)	0.70583 (5)	0.0198 (4)
H201	0.2028	0.2117	0.7152	0.030*
H200	0.2437	0.0873	0.7012	0.030*

Atomic displacement parameters (Å²)

	U^{11}	U^{22}	U^{33}	U^{12}	U^{13}	U^{23}
C11C	0.0075 (12)	0.0134 (13)	0.0155 (12)	−0.0018 (11)	0.0009 (9)	−0.0015 (11)
C12C	0.0224 (15)	0.0148 (14)	0.0131 (13)	−0.0038 (12)	0.0015 (11)	−0.0004 (11)
C13C	0.0316 (17)	0.0126 (15)	0.0236 (15)	−0.0063 (13)	0.0016 (13)	0.0001 (12)
C14C	0.0205 (14)	0.0135 (14)	0.0289 (15)	−0.0057 (13)	0.0027 (12)	−0.0048 (12)
C15C	0.0151 (13)	0.0203 (15)	0.0146 (12)	0.0007 (12)	0.0022 (11)	−0.0075 (11)
C16C	0.0131 (12)	0.0150 (14)	0.0160 (13)	−0.0014 (12)	0.0023 (10)	0.0001 (11)
N11	0.0135 (10)	0.0099 (11)	0.0102 (10)	−0.0007 (9)	−0.0004 (8)	0.0002 (8)
N12	0.0145 (11)	0.0108 (11)	0.0104 (10)	−0.0001 (9)	−0.0002 (9)	−0.0004 (8)
C13	0.0084 (12)	0.0113 (13)	0.0135 (12)	0.0001 (10)	−0.0013 (10)	−0.0003 (10)
C14	0.0120 (13)	0.0099 (13)	0.0111 (11)	0.0008 (11)	0.0002 (10)	0.0018 (10)
C14A	0.0110 (12)	0.0099 (13)	0.0102 (11)	0.0019 (10)	0.0007 (10)	0.0005 (10)
C15	0.0193 (13)	0.0084 (13)	0.0083 (11)	−0.0016 (11)	0.0015 (10)	−0.0011 (10)
N16	0.0166 (11)	0.0098 (11)	0.0088 (10)	−0.0024 (9)	0.0011 (9)	−0.0017 (8)
C17	0.0129 (12)	0.0102 (13)	0.0099 (12)	0.0002 (11)	−0.0017 (10)	0.0007 (10)
O17	0.0229 (10)	0.0117 (9)	0.0101 (8)	−0.0038 (8)	0.0000 (8)	0.0019 (7)
N18	0.0185 (11)	0.0116 (11)	0.0076 (10)	−0.0033 (10)	0.0017 (9)	0.0016 (8)
C18A	0.0096 (11)	0.0101 (13)	0.0093 (11)	−0.0001 (10)	0.0006 (10)	0.0004 (10)
C11′	0.0176 (13)	0.0106 (13)	0.0091 (11)	−0.0021 (11)	−0.0013 (10)	0.0003 (10)
C12′	0.0146 (13)	0.0125 (13)	0.0107 (11)	0.0028 (11)	−0.0008 (10)	−0.0002 (10)
C13′	0.0151 (13)	0.0111 (13)	0.0111 (12)	−0.0009 (11)	0.0013 (10)	−0.0018 (10)
O13′	0.0249 (11)	0.0156 (10)	0.0203 (10)	0.0006 (9)	0.0010 (9)	−0.0096 (8)
C14′	0.0134 (13)	0.0147 (13)	0.0093 (12)	−0.0010 (11)	−0.0021 (10)	−0.0009 (10)
O14′	0.0139 (9)	0.0212 (10)	0.0081 (8)	0.0012 (8)	0.0002 (7)	0.0021 (7)
C15′	0.0147 (13)	0.0152 (14)	0.0140 (12)	0.0031 (11)	0.0017 (10)	−0.0011 (11)
O15′	0.0157 (10)	0.0185 (11)	0.0219 (10)	0.0053 (9)	−0.0026 (8)	−0.0070 (8)
O100	0.0151 (9)	0.0221 (11)	0.0170 (9)	0.0012 (9)	−0.0005 (8)	−0.0057 (8)
C21C	0.0101 (12)	0.0104 (13)	0.0136 (12)	0.0011 (10)	−0.0023 (10)	−0.0015 (10)
C22C	0.0163 (13)	0.0140 (14)	0.0122 (12)	0.0017 (11)	−0.0019 (10)	0.0004 (10)
C23C	0.0147 (13)	0.0132 (14)	0.0197 (14)	0.0003 (12)	0.0001 (11)	0.0024 (11)
C24C	0.0150 (13)	0.0101 (14)	0.0234 (14)	−0.0015 (11)	0.0013 (11)	−0.0046 (11)

C25C	0.0143 (13)	0.0157 (14)	0.0148 (12)	0.0009 (12)	0.0005 (11)	−0.0046 (11)
C26C	0.0114 (12)	0.0150 (13)	0.0136 (12)	−0.0003 (11)	0.0003 (10)	−0.0021 (11)
N21	0.0187 (12)	0.0111 (11)	0.0123 (10)	−0.0004 (10)	−0.0020 (9)	−0.0007 (9)
N22	0.0154 (11)	0.0125 (12)	0.0132 (10)	0.0012 (10)	−0.0013 (9)	−0.0019 (9)
C23	0.0096 (11)	0.0118 (13)	0.0109 (11)	0.0024 (11)	−0.0012 (10)	0.0002 (10)
C24	0.0132 (13)	0.0111 (13)	0.0113 (12)	0.0013 (11)	0.0022 (10)	0.0017 (10)
C24A	0.0105 (12)	0.0119 (13)	0.0107 (11)	0.0002 (11)	0.0010 (10)	0.0007 (10)
C25	0.0176 (13)	0.0088 (13)	0.0105 (12)	−0.0019 (11)	−0.0016 (10)	0.0017 (10)
N26	0.0188 (11)	0.0094 (11)	0.0082 (9)	−0.0021 (10)	0.0005 (9)	−0.0008 (8)
C27	0.0143 (13)	0.0127 (14)	0.0108 (12)	0.0001 (11)	0.0022 (10)	−0.0004 (10)
O27	0.0314 (12)	0.0104 (10)	0.0114 (9)	−0.0039 (9)	0.0004 (8)	0.0011 (8)
N28	0.0261 (12)	0.0110 (11)	0.0077 (10)	−0.0024 (10)	0.0012 (9)	0.0028 (9)
C28A	0.0137 (12)	0.0090 (13)	0.0120 (12)	0.0008 (10)	0.0002 (10)	−0.0002 (10)
C21′	0.0170 (13)	0.0136 (14)	0.0110 (12)	−0.0012 (12)	0.0009 (10)	−0.0013 (10)
C22′	0.0135 (13)	0.0199 (15)	0.0103 (12)	−0.0014 (11)	0.0000 (10)	−0.0003 (11)
C23′	0.0164 (13)	0.0119 (13)	0.0070 (11)	−0.0036 (11)	−0.0003 (10)	−0.0016 (10)
O23′	0.0158 (9)	0.0239 (11)	0.0071 (8)	0.0016 (9)	−0.0005 (7)	0.0016 (8)
O24′	0.0160 (9)	0.0210 (10)	0.0108 (9)	0.0066 (9)	0.0011 (7)	0.0028 (8)
C24′	0.0186 (13)	0.0166 (14)	0.0069 (11)	0.0015 (12)	−0.0004 (10)	−0.0008 (10)
C25′	0.0156 (14)	0.0306 (17)	0.0128 (13)	−0.0031 (13)	0.0020 (11)	−0.0050 (12)
O25′	0.0251 (12)	0.0359 (13)	0.0194 (10)	−0.0166 (10)	0.0046 (9)	−0.0068 (9)
O200	0.0159 (10)	0.0172 (10)	0.0264 (10)	−0.0021 (9)	−0.0005 (8)	−0.0024 (8)

Geometric parameters (Å, º)

C11C—C12C	1.396 (4)	C21C—C22C	1.393 (4)
C11C—C16C	1.401 (4)	C21C—C26C	1.400 (3)
C11C—C13	1.483 (4)	C21C—C23	1.486 (4)
C12C—C13C	1.387 (4)	C22C—C23C	1.391 (4)
C12C—H12C	0.9500	C22C—H22C	0.9500
C13C—C14C	1.380 (4)	C23C—C24C	1.384 (4)
C13C—H13C	0.9500	C23C—H23C	0.9500
C14C—C15C	1.389 (4)	C24C—C25C	1.383 (4)
C14C—H14C	0.9500	C24C—H24C	0.9500
C15C—C16C	1.383 (4)	C25C—C26C	1.384 (4)
C15C—H15C	0.9500	C25C—H25C	0.9500
C16C—H16C	0.9500	C26C—H26C	0.9500
N11—C18A	1.327 (3)	N21—C28A	1.322 (3)
N11—N12	1.349 (3)	N21—N22	1.344 (3)
N12—C13	1.328 (3)	N22—C23	1.337 (3)
C13—C14	1.419 (3)	C23—C24	1.409 (3)
C14—C14A	1.351 (4)	C24—C24A	1.360 (4)
C14—H14	0.9500	C24—H24	0.9500
C14A—C18A	1.401 (3)	C24A—C28A	1.399 (3)
C14A—C15	1.499 (3)	C24A—C25	1.495 (3)
C15—N16	1.465 (3)	C25—N26	1.463 (3)
C15—H15E	0.9900	C25—H25D	0.9900
C15—H15D	0.9900	C25—H25E	0.9900

N16—C17	1.365 (3)	N26—C27	1.367 (3)
N16—C11′	1.457 (3)	N26—C21′	1.448 (3)
C17—O17	1.237 (3)	C27—O27	1.232 (3)
C17—N18	1.368 (3)	C27—N28	1.358 (3)
N18—C18A	1.375 (3)	N28—C28A	1.379 (3)
N18—H18N	0.8800	N28—H28N	0.8800
C11′—O14′	1.432 (3)	C21′—O24′	1.441 (3)
C11′—C12′	1.523 (3)	C21′—C22′	1.533 (4)
C11′—H11′	1.0000	C21′—H21′	1.0000
C12′—C13′	1.522 (3)	C22′—C23′	1.522 (3)
C12′—H12A	0.9900	C22′—H22A	0.9900
C12′—H12B	0.9900	C22′—H22B	0.9900
C13′—O13′	1.425 (3)	C23′—O23′	1.423 (3)
C13′—C14′	1.528 (4)	C23′—C24′	1.519 (4)
C13′—H13′	1.0000	C23′—H23′	1.0000
O13′—H13O	0.8400	O23′—H23O	0.8400
C14′—O14′	1.440 (3)	O24′—C24′	1.441 (3)
C14′—C15′	1.508 (4)	C24′—C25′	1.503 (4)
C14′—H14′	1.0000	C24′—H24′	1.0000
C15′—O15′	1.431 (3)	C25′—O25′	1.422 (3)
C15′—H15A	0.9900	C25′—H25A	0.9900
C15′—H15B	0.9900	C25′—H25B	0.9900
O15′—H15O	0.8400	O25′—H25O	0.8400
O100—H101	0.9600	O200—H201	0.9600
O100—H100	0.9602	O200—H200	0.9601

C12C—C11C—C16C	118.0 (2)	C22C—C21C—C26C	118.4 (2)
C12C—C11C—C13	121.0 (2)	C22C—C21C—C23	120.8 (2)
C16C—C11C—C13	121.0 (2)	C26C—C21C—C23	120.7 (2)
C13C—C12C—C11C	120.9 (2)	C23C—C22C—C21C	120.9 (2)
C13C—C12C—H12C	119.6	C23C—C22C—H22C	119.6
C11C—C12C—H12C	119.6	C21C—C22C—H22C	119.6
C14C—C13C—C12C	120.5 (3)	C24C—C23C—C22C	120.0 (2)
C14C—C13C—H13C	119.8	C24C—C23C—H23C	120.0
C12C—C13C—H13C	119.8	C22C—C23C—H23C	120.0
C13C—C14C—C15C	119.5 (3)	C25C—C24C—C23C	119.7 (2)
C13C—C14C—H14C	120.3	C25C—C24C—H24C	120.1
C15C—C14C—H14C	120.3	C23C—C24C—H24C	120.1
C16C—C15C—C14C	120.3 (2)	C24C—C25C—C26C	120.6 (2)
C16C—C15C—H15C	119.8	C24C—C25C—H25C	119.7
C14C—C15C—H15C	119.8	C26C—C25C—H25C	119.7
C15C—C16C—C11C	120.8 (2)	C25C—C26C—C21C	120.5 (2)
C15C—C16C—H16C	119.6	C25C—C26C—H26C	119.8
C11C—C16C—H16C	119.6	C21C—C26C—H26C	119.8
C18A—N11—N12	119.1 (2)	C28A—N21—N22	118.9 (2)
C13—N12—N11	120.5 (2)	C23—N22—N21	120.9 (2)
N12—C13—C14	121.2 (2)	N22—C23—C24	120.4 (2)
N12—C13—C11C	116.5 (2)	N22—C23—C21C	116.8 (2)

C14—C13—C11C	122.2 (2)	C24—C23—C21C	122.7 (2)
C14A—C14—C13	118.6 (2)	C24A—C24—C23	119.3 (2)
C14A—C14—H14	120.7	C24A—C24—H24	120.4
C13—C14—H14	120.7	C23—C24—H24	120.4
C14—C14A—C18A	117.1 (2)	C24—C24A—C28A	116.3 (2)
C14—C14A—C15	123.1 (2)	C24—C24A—C25	123.6 (2)
C18A—C14A—C15	119.8 (2)	C28A—C24A—C25	120.1 (2)
N16—C15—C14A	112.7 (2)	N26—C25—C24A	112.8 (2)
N16—C15—H15E	109.1	N26—C25—H25D	109.0
C14A—C15—H15E	109.1	C24A—C25—H25D	109.0
N16—C15—H15D	109.1	N26—C25—H25E	109.0
C14A—C15—H15D	109.1	C24A—C25—H25E	109.0
H15E—C15—H15D	107.8	H25D—C25—H25E	107.8
C17—N16—C11′	117.5 (2)	C27—N26—C21′	117.2 (2)
C17—N16—C15	123.1 (2)	C27—N26—C25	125.2 (2)
C11′—N16—C15	115.87 (19)	C21′—N26—C25	117.0 (2)
O17—C17—N16	122.6 (2)	O27—C27—N28	120.5 (2)
O17—C17—N18	119.7 (2)	O27—C27—N26	122.3 (2)
N16—C17—N18	117.7 (2)	N28—C27—N26	117.2 (2)
C17—N18—C18A	124.5 (2)	C27—N28—C28A	124.5 (2)
C17—N18—H18N	117.8	C27—N28—H28N	117.7
C18A—N18—H18N	117.8	C28A—N28—H28N	117.7
N11—C18A—N18	117.3 (2)	N21—C28A—N28	116.6 (2)
N11—C18A—C14A	123.4 (2)	N21—C28A—C24A	123.8 (2)
N18—C18A—C14A	119.3 (2)	N28—C28A—C24A	119.6 (2)
O14′—C11′—N16	108.5 (2)	O24′—C21′—N26	107.7 (2)
O14′—C11′—C12′	106.55 (19)	O24′—C21′—C22′	105.87 (19)
N16—C11′—C12′	115.0 (2)	N26—C21′—C22′	115.7 (2)
O14′—C11′—H11′	108.9	O24′—C21′—H21′	109.1
N16—C11′—H11′	108.9	N26—C21′—H21′	109.1
C12′—C11′—H11′	108.9	C22′—C21′—H21′	109.1
C13′—C12′—C11′	103.2 (2)	C23′—C22′—C21′	105.2 (2)
C13′—C12′—H12A	111.1	C23′—C22′—H22A	110.7
C11′—C12′—H12A	111.1	C21′—C22′—H22A	110.7
C13′—C12′—H12B	111.1	C23′—C22′—H22B	110.7
C11′—C12′—H12B	111.1	C21′—C22′—H22B	110.7
H12A—C12′—H12B	109.1	H22A—C22′—H22B	108.8
O13′—C13′—C12′	112.0 (2)	O23′—C23′—C24′	113.4 (2)
O13′—C13′—C14′	108.0 (2)	O23′—C23′—C22′	109.1 (2)
C12′—C13′—C14′	102.44 (19)	C24′—C23′—C22′	103.3 (2)
O13′—C13′—H13′	111.3	O23′—C23′—H23′	110.3
C12′—C13′—H13′	111.3	C24′—C23′—H23′	110.3
C14′—C13′—H13′	111.3	C22′—C23′—H23′	110.3
C13′—O13′—H13O	109.5	C23′—O23′—H23O	109.5
O14′—C14′—C15′	110.8 (2)	C24′—O24′—C21′	110.73 (18)
O14′—C14′—C13′	106.2 (2)	O24′—C24′—C25′	108.3 (2)
C15′—C14′—C13′	111.3 (2)	O24′—C24′—C23′	104.78 (19)
O14′—C14′—H14′	109.5	C25′—C24′—C23′	115.9 (2)

C15′—C14′—H14′	109.5	O24′—C24′—H24′	109.2
C13′—C14′—H14′	109.5	C25′—C24′—H24′	109.2
C11′—O14′—C14′	110.27 (18)	C23′—C24′—H24′	109.2
O15′—C15′—C14′	112.2 (2)	O25′—C25′—C24′	109.9 (2)
O15′—C15′—H15A	109.2	O25′—C25′—H25A	109.7
C14′—C15′—H15A	109.2	C24′—C25′—H25A	109.7
O15′—C15′—H15B	109.2	O25′—C25′—H25B	109.7
C14′—C15′—H15B	109.2	C24′—C25′—H25B	109.7
H15A—C15′—H15B	107.9	H25A—C25′—H25B	108.2
C15′—O15′—H15O	109.5	C25′—O25′—H25O	109.5
H101—O100—H100	105.0	H201—O200—H200	105.0

C16C—C11C—C12C—C13C	−0.4 (4)	C26C—C21C—C22C—C23C	0.0 (4)
C13—C11C—C12C—C13C	−179.8 (3)	C23—C21C—C22C—C23C	−179.3 (2)
C11C—C12C—C13C—C14C	0.7 (5)	C21C—C22C—C23C—C24C	−0.3 (4)
C12C—C13C—C14C—C15C	−0.2 (5)	C22C—C23C—C24C—C25C	0.0 (4)
C13C—C14C—C15C—C16C	−0.5 (4)	C23C—C24C—C25C—C26C	0.7 (4)
C14C—C15C—C16C—C11C	0.8 (4)	C24C—C25C—C26C—C21C	−1.0 (4)
C12C—C11C—C16C—C15C	−0.4 (4)	C22C—C21C—C26C—C25C	0.6 (4)
C13—C11C—C16C—C15C	179.1 (2)	C23—C21C—C26C—C25C	179.9 (2)
C18A—N11—N12—C13	0.6 (3)	C28A—N21—N22—C23	−0.6 (4)
N11—N12—C13—C14	−1.5 (4)	N21—N22—C23—C24	4.4 (4)
N11—N12—C13—C11C	179.7 (2)	N21—N22—C23—C21C	−176.5 (2)
C12C—C11C—C13—N12	163.4 (2)	C22C—C21C—C23—N22	172.4 (2)
C16C—C11C—C13—N12	−16.1 (4)	C26C—C21C—C23—N22	−6.8 (4)
C12C—C11C—C13—C14	−15.4 (4)	C22C—C21C—C23—C24	−8.5 (4)
C16C—C11C—C13—C14	165.1 (2)	C26C—C21C—C23—C24	172.2 (2)
N12—C13—C14—C14A	0.2 (4)	N22—C23—C24—C24A	−3.2 (4)
C11C—C13—C14—C14A	179.0 (2)	C21C—C23—C24—C24A	177.8 (2)
C13—C14—C14A—C18A	1.8 (4)	C23—C24—C24A—C28A	−1.6 (4)
C13—C14—C14A—C15	−177.2 (2)	C23—C24—C24A—C25	176.5 (2)
C14—C14A—C15—N16	−167.1 (2)	C24—C24A—C25—N26	176.0 (2)
C18A—C14A—C15—N16	13.9 (3)	C28A—C24A—C25—N26	−6.1 (3)
C14A—C15—N16—C17	−20.9 (3)	C24A—C25—N26—C27	−0.6 (4)
C14A—C15—N16—C11′	−179.2 (2)	C24A—C25—N26—C21′	−171.4 (2)
C11′—N16—C17—O17	−8.2 (4)	C21′—N26—C27—O27	−3.3 (4)
C15—N16—C17—O17	−166.1 (2)	C25—N26—C27—O27	−174.1 (3)
C11′—N16—C17—N18	173.7 (2)	C21′—N26—C27—N28	177.3 (2)
C15—N16—C17—N18	15.7 (4)	C25—N26—C27—N28	6.5 (4)
O17—C17—N18—C18A	179.4 (2)	O27—C27—N28—C28A	174.4 (3)
N16—C17—N18—C18A	−2.4 (4)	N26—C27—N28—C28A	−6.2 (4)
N12—N11—C18A—N18	−179.3 (2)	N22—N21—C28A—N28	176.2 (2)
N12—N11—C18A—C14A	1.6 (4)	N22—N21—C28A—C24A	−4.5 (4)
C17—N18—C18A—N11	177.2 (2)	C27—N28—C28A—N21	179.0 (2)
C17—N18—C18A—C14A	−3.7 (4)	C27—N28—C28A—C24A	−0.3 (4)
C14—C14A—C18A—N11	−2.8 (4)	C24—C24A—C28A—N21	5.5 (4)
C15—C14A—C18A—N11	176.2 (2)	C25—C24A—C28A—N21	−172.6 (2)
C14—C14A—C18A—N18	178.1 (2)	C24—C24A—C28A—N28	−175.2 (2)

C15—C14A—C18A—N18	−2.9 (4)	C25—C24A—C28A—N28	6.7 (4)
C17—N16—C11′—O14′	−97.5 (3)	C27—N26—C21′—O24′	−103.8 (3)
C15—N16—C11′—O14′	62.0 (3)	C25—N26—C21′—O24′	67.8 (3)
C17—N16—C11′—C12′	143.3 (2)	C27—N26—C21′—C22′	138.1 (2)
C15—N16—C11′—C12′	−57.1 (3)	C25—N26—C21′—C22′	−50.3 (3)
O14′—C11′—C12′—C13′	26.9 (3)	O24′—C21′—C22′—C23′	−11.4 (3)
N16—C11′—C12′—C13′	147.1 (2)	N26—C21′—C22′—C23′	107.7 (2)
C11′—C12′—C13′—O13′	82.3 (2)	C21′—C22′—C23′—O23′	147.3 (2)
C11′—C12′—C13′—C14′	−33.2 (3)	C21′—C22′—C23′—C24′	26.3 (3)
O13′—C13′—C14′—O14′	−89.8 (2)	N26—C21′—O24′—C24′	−133.6 (2)
C12′—C13′—C14′—O14′	28.6 (2)	C22′—C21′—O24′—C24′	−9.2 (3)
O13′—C13′—C14′—C15′	149.5 (2)	C21′—O24′—C24′—C25′	150.6 (2)
C12′—C13′—C14′—C15′	−92.1 (2)	C21′—O24′—C24′—C23′	26.2 (3)
N16—C11′—O14′—C14′	−133.5 (2)	O23′—C23′—C24′—O24′	−149.9 (2)
C12′—C11′—O14′—C14′	−9.2 (3)	C22′—C23′—C24′—O24′	−31.9 (2)
C15′—C14′—O14′—C11′	108.6 (2)	O23′—C23′—C24′—C25′	90.7 (3)
C13′—C14′—O14′—C11′	−12.4 (3)	C22′—C23′—C24′—C25′	−151.3 (2)
O14′—C14′—C15′—O15′	59.2 (3)	O24′—C24′—C25′—O25′	−63.0 (3)
C13′—C14′—C15′—O15′	177.20 (19)	C23′—C24′—C25′—O25′	54.4 (3)

Hydrogen-bond geometry (Å, º)

D—H···*A*	*D*—H	H···*A*	*D*···*A*	*D*—H···*A*
N18—H18*N*···O27^{i}	0.88	1.92	2.773 (3)	162
O13′—H13*O*···O17^{ii}	0.84	2.15	2.968 (3)	166
O15′—H15*O*···O100	0.84	1.91	2.736 (2)	169
O100—H101···O15′^{iii}	0.96	1.86	2.781 (3)	160
O100—H100···N22	0.96	1.99	2.946 (3)	175
N28—H28*N*···O17^{iv}	0.88	1.95	2.823 (3)	173
O23′—H23*O*···N11^{v}	0.84	2.05	2.846 (3)	158
O25′—H25*O*···O200^{vi}	0.84	1.90	2.721 (3)	164
O200—H201···O24′^{vii}	0.96	1.84	2.801 (3)	175
O200—H200···O23′	0.96	1.89	2.836 (3)	169

Symmetry codes: (i) *x*, *y*+1, *z*; (ii) *x*−1/2, −*y*+3/2, −*z*+2; (iii) *x*−1/2, −*y*+1/2, −*z*+2; (iv) *x*, *y*−1, *z*; (v) −*x*+1, *y*−1/2, −*z*+3/2; (vi) *x*+1, *y*, *z*; (vii) −*x*+1, *y*+1/2, −*z*+3/2.